Polarized FT-IR Study of Macroscopically Oriented Electrospun Nylon-6 Nanofibers

Keun-Hyung Lee,[†,‡] Kwan-Woo Kim,[§] Andrea Pesapane,[†] Hak-Yong Kim,*[,§] and John F. Rabolt*[,†]

Department of Materials Science and Engineering, University of Delaware, Newark, Delaware 19716; Collaborative Innovation Center for Nanotech Fiber, Faculty of Textile Science and Technology, Shinshu University, Ueda, Nagano 386-8567, Japan; and Department of Textile Engineering, Chonbuk National University, Jeonju 561-756, Republic of Korea

Received August 27, 2007; Revised Manuscript Received December 9, 2007

ABSTRACT: Randomly deposited or partially aligned electrospun nylon-6 nanofibers were prepared by using a rotating collector with linear velocity from 0 to 900 m/min, and their molecular orientation was characterized with polarized Fourier-transform infrared (FT-IR) spectroscopy. At a linear velocity of 0 m/min, electrospun nylon-6 nanofibers are randomly deposited onto a collector owing to the bending instability of the charged jet. In this case the parallel polarized FT-IR spectrum (obtained at two mutually perpendicular directions) is the same as the perpendicular polarized spectrum, indicating that there is no molecular orientation in the electropun membrane. When the linear velocity of the collector was increased from 0 to 300 m/min, several changes in IR band intensity are observed, including the NH stretching band at 3303 cm^{-1} and the amide I and II vibrations (1647 and 1543 cm^{-1}, respectively) in the two polarized FTIR spectra. Also, the intensity of the amide II vibration is observed to gradually increase in the parallel polarized FT-IR spectrum, with an increase in the linear velocity of the collector, whereas its intensity is observed to decrease in the perpendicularly polarized spectrum. This indicates that the polymer chains are preferentially oriented along the fiber axis. Also, a decrease in the average fiber diameter (from 250 to 125 nm) is observed in SEM micrographs, indicating that the fibers are stretched and aligned by the high-speed rotating collector.

Introduction

Nylon-6 is widely used as an engineering polymer, especially for fiber and film manufacturing.[1] It is well-known that nylon-6 has two different crystalline structures, α- and γ-forms. The conformation of the α-form is a fully extended planar zigzag and is thermodynamically stable, whereas the γ-form adopts a helical or kinked structure and is metastable.[2] Since all nylon-6 amide bonds lie in the same direction (perpendicular to the polymer chain axis), nylon-6 is very similar in structure to the β-sheet conformation of natural polypeptides.

Electrospinning is a fiber spinning technique that employs a high-voltage supply together with a polymeric solution or melt that can produce polymer fibers with diameters ranging from several microns to nanometers.[3−5] Thus far, a wide variety of organic polymers have been successfully prepared via the electrospinning process.[6,7] Recently, there has been an increased interest in the macroscopic alignment of electrospun fibers for many applications, ranging from electrical and optical applications to biomedical applications.

Macroscopically aligned electrospun fibers have been obtained by modifying the fiber collection system to incorporate a high-speed rotating drum,[8−10] a copper wire drum,[11] a scanning tip,[12] or conductive plates containing an insulating gap.[13] However, very limited work on the molecular orientation of polymer chains within these macroscopically aligned electrospun fibers exists.[10,14]

In this study, the electrospun nylon-6 nanofibers were deposited on a rotating collector with different linear velocities, which induced partial molecular orientation and macroscopic fiber alignment. The mechanism of molecular alignment of polymer chains in nanofibers was examined in detail using polarized FT-IR spectroscopy. The use of this technique to characterize polymers and their overall molecular orientation has been well documented.[15−17]

Experimental Section

Nylon-6 pellets (relative viscosity of 2.8) used in this study were obtained from Kolon Industries (Republic of Korea). The pellets were dissolved in formic acid at room temperature and electrospun onto a rotating metallic mandrel capable of rotating up to 3000 m/min. Aligned nylon-6 nanofibers were prepared with varying degrees of molecular alignment by controlling the linear velocity of the mandrel surface (0, 300, 600, and 900 m/min). Electrospinning was carried out using a nylon-6 concentration of 22 wt % in formic acid solution, with an applied voltage of 22 kV and a tip-to-collector distance of 12 cm. A schematic of the electrospinning apparatus is shown in Figure 1. After electrospinning, the nylon-6 nanofibers were placed under vacuum to remove the residual solvent.

The morphology of electrospun nylon-6 nanofibers was examined with scanning electron microscope (SEM, JEOL JSM-5900, Japan). To monitor the changes in the molecular orientation as a function of a linear velocity of the rotating mandrel, a Fourier transform infrared spectrometer (FT-IR, Nexus 670, Thermo Nicolet) with a ZnSe polarizer was used. The spectra were recorded from 500 to 4000 cm^{-1} with a 4 cm^{-1} resolution and the coaddition of 128 scans. In the parallel polarization, the direction of the oscillating electric field of the incident IR beam is parallel to the machine direction of collection of the fibers (parallel to the fiber axis) while in the perpendicular polarization it is perpendicular to the machine direction (perpendicular to the fiber axis). Thermal measurements

* Corresponding authors. J.F.R.: e-mail rabolt@udel.edu, phone 1-302-831-4476, Fax 1-302-831-4545. H.-Y.K.: e-mail khy@chonbuk.ac.kr, phone 82-63-270-2351, Fax 82-63-270-2348.
† University of Delaware.
‡ Shinshu University.
§ Chonbuk National University.

10.1021/ma701927w CCC: $40.75
Published on Web 01/26/2008

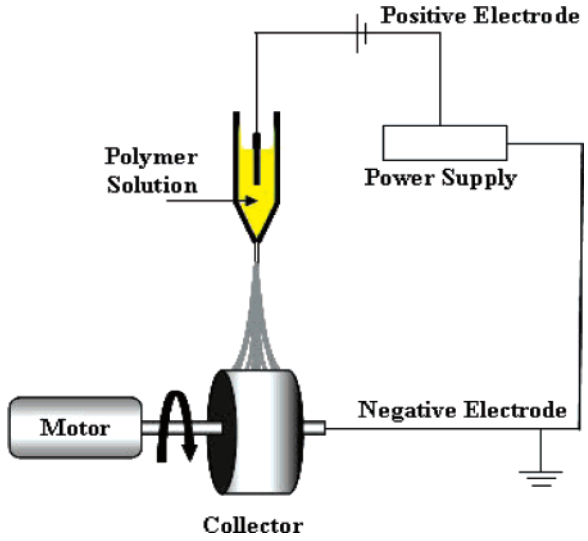

Figure 1. Schematic diagram of electrospinning setup and collection system.

were performed with a DSC (Q100 TA Instruments) operating at a heating rate of 20 °C/min under a N_2 atmosphere. Crystallinity (X_c) values were determined using the ratio of $\Delta H_f/\Delta H°_f$, where ΔH_f is the measured DSC heat of fusion (J/g) and $\Delta H°_f$ is the heat of fusion for a 100% nylon-6 crystal. A value of $\Delta H°_f = 240$ J/g[18] was used to calculate the degree of crystallinity.

Results and Discussion

In electrospinning, it has been shown that the viscosity or concentration plays a major role in determining the morphology and diameter of electrospun fibers.[19] As demonstrated by SEM micrographs shown in Figure 2, nanofibers with different diameters result when the mandrel speed is increased even though all samples are electrospun from the same polymer concentration (22 wt % in formic acid). At a mandrel linear velocity of 0 m/min, electrospun nylon-6 nanofibers are randomly deposited onto the collector due to the bending instability of the charged jet (Figure 2A).[20] On the other hand, partially aligned nylon-6 nanofibers were prepared by adjusting the linear velocity of the collector (Figure 2B), with better alignment occurring as this linear velocity approached that of the electrospinning speed. The frequency distribution of the observed nylon-6 fiber diameters deposited onto the collector with a linear velocity of 0 and 300 m/min is illustrated in parts C and D of Figure 2, respectively. As the linear velocity of the mandrel is increased from 0 to 300 m/min, the average diameter decreases from 250 to 125 nm, indicating that the fibers are stretched and aligned toward to rollup direction. For larger linear velocities, the average fiber diameter showed only small additional changes (data not shown).

As mentioned above, the molecular structure of nylon-6 consists of amide groups (CO−NH) separated by linear chains of methylene units [−$(CH_2)_5$−]. All amide groups are oriented approximately perpendicular to the polymer chain axis and form intermolecular hydrogen bonds. There are two possible crystalline forms for nylon-6: the parallel chain α-form and antiparallel chain γ-form. The IR bands have been assigned previously[15,17] and are presented in Table 1.

When the nylon-6 nanofibers are randomly collected (linear velocity of 0 m/min), the IR spectra obtained in any two perpendicular directions are exactly the same (data not shown), indicating that there is no macroscopic fiber orientation when the nylon-6 nanofibers are collected on a nonrotating mandrel collector surface. However, as soon as the linear velocity of collector is increased to 300 m/min, several changes in the two polarized IR spectra obtained with polarization along the axes of the aligned fibers and perpendicular to the axes of the aligned fibers were observed (Figure 3). Although the most obvious changes are in the N−H stretching region, the amide I and the amide II regions due to the strong intensity changes observed for these bands, the entire spectrum is strongly affected by an increase in the linear velocity of the mandrel.

Parallel and perpendicular polarized FT-IR spectra as a function of the linear velocity of the collector are shown in Figures 4 and 5, respectively. As the linear velocity of collector is increased, the relative band intensities of amide I, amide II, amide III, and CC stretching are observed to change in the polarized FT-IR spectra. In particular, amide II is strongly affected by the linear velocity of the collector (see inset in Figures 4 and 5) due to the fact that the molecular orientation is increased with linear velocity of the collector. Characterization of molecular orientation is commonly demonstrated by calculating the dichroic ratio of different vibrational bands from the observed IR spectra. The dichroic ratio can be calculated using the expression $R = P_{\parallel}/P_{\perp}$, where R is the dichroic ratio, $P_{\parallel}$ the parallel-polarized infrared absorbance intensity, and $P_{\perp}$ the perpendicularly-polarized infrared absorbance intensity for a particular vibration. For a randomly oriented sample, R is equal to 1 (equal infrared absorbance intensity in two mutually perpendicular directions), while for a uniaxially oriented sample (all polymer chains aligned along the fiber axis and a change in dipole moment of a particular vibration that is aligned along the fiber axis), R equals infinity. The dichroic ratios for the IR bands observed as a function of the linear velocity of the rotating collector are summarized in Table 2. (Absorbance for the bands at 929 and 974 cm^{-1} was calculated using a curve fitting routine in Origin 7.5 software because these are not isolated bands and needed to first be resolved.)

As expected, the amide I band at 1645 cm^{-1} (primarily due to the carbonyl stretching vibration) shows perpendicular polarization as do the NH stretching and the CONH in-plane vibration attributed to the γ-form at 974 cm^{-1} (Figures 5 and 6).[17] On the other hand, the amide II band mainly attributable to CN stretching and NH in-plane bending shows parallel polarization. The CC stretching band at 1121 cm^{-1}, characteristic of the amorphous phase,[17] and the CONH in-plane vibration attributable to the α-form at 929 cm^{-1} (Figures 4 and 6) also exhibit parallel polarization. Hence, it is clear that the molecular orientation of nylon-6 is influenced by the linear velocity of the collector as evidenced by the polarized IR data. However, it is interesting to note that the opposite polarization behavior is observed for the CONH vibration of the two different crystalline forms. In the α-form the amide group lies in the same plane as the aliphatic carbon chain while in the γ-form the amide group is twisted about 60° out of this plane in support of the observed change in polarization behavior.[2] From the SEM micrographs, it is also evident that there is a large decrease in the average fiber diameter, which occurred at the 300 m/min windup speed while only small additional changes in the average fiber diameter occurs with higher windup speeds.

At the same time the dichroic ratio, for all the different bands, indicates that the orientation continues to increase as the windup speed reaches 900 m/min. This observation could be understood if one considers that the increase in windup speed increases the molecular alignment of polymer chains within the fibers while also improving the macroscopic alignment of the fibers simultaneously. A moderate increase in macroscopic fiber alignment

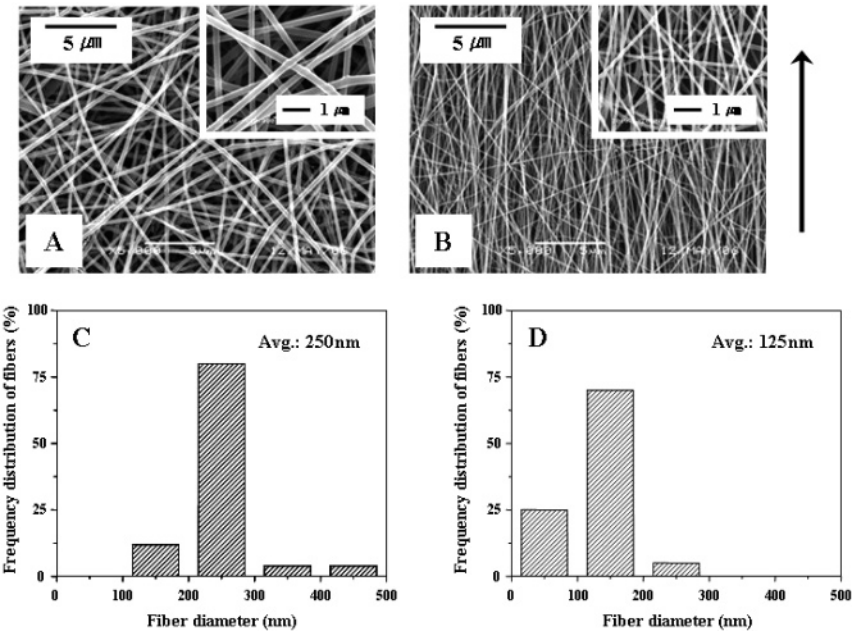

Figure 2. SEM images and frequency distribution of nylon-6 nanofiber diameters of electrospun fibers obtained at two distinct linear velocities of the rotating mandrel: (A, C) 0 and (B, D) 300 m/min. Arrow indicates the draw direction.

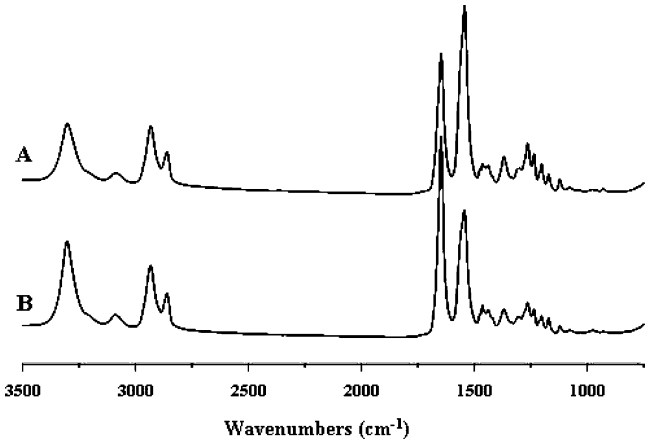

Figure 3. Polarized FT-IR spectra of nylon-6 nanofibers electrospun onto the rotating mandrel collector with a linear velocity of 300 m/min. (A) parallel and (B) perpendicular to the axes of the macroscopically aligned fibers.

Table 1. FT-IR Band Assignments of Nylon-6

band (cm^{-1})	assignment
3300	hydrogen-bonded NH stretching
3086	NH Fermi resonance
2931	CH_2 asymmetric stretching
2859	CH_2 symmetric stretching
1645	amide I
1544	amide II
1369	amide III + CH_2 wagging
1264	amide III + CH_2 wagging
1236	CH_2 wagging/twisting
1203	amide III + CH_2 wagging
1170	CONH skeletal motion
1121	CC stretching (amorphous)
1078	CC stretching
974	CONH in-plane (γ)
929	CONH in-plane (α)

is observed from SEM micrographs (data not shown) as the windup speed is increased from 300 to 900 m/min.

It is impossible to affirm the exact crystallinity of the sample and/or quantify the α and γ content using only IR spectroscopy. Comparing the relative absorbance of the 1121, 974, and 929

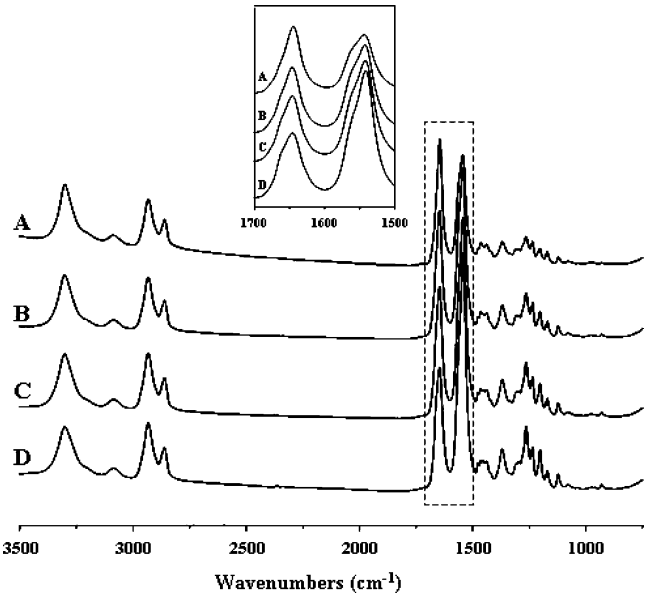

Figure 4. Parallel polarized FT-IR spectra of nylon-6 nanofibers electrospun onto the rotating mandrel collector with a linear velocity of (A) 0, (B) 300, (C) 600, and (D) 900 m/min.

cm^{-1} bands in the unpolarized spectra (data not shown), it is possible to conclude that there is a slight increase in crystallinity with an increase in the windup speed at the collector. Concomitantly, there is a pronounced increase in the concentration of α-form, which becomes more evident as the windup speed increases from 0 to 300 m/min. This is supported by band shifts in the CH_2 stretching region (Figure 7). These vibrational bands contain contributions from both the amorphous and the crystalline regions. It has been reported that the CH_2 stretching frequencies of the α-form are found at higher positions because the polymer chains are more tightly packed in this form and the CH bond is shorter.[21] In our experiments, both the CH_2 symmetric and CH_2 asymmetric stretching bands have shifted slightly to higher wavenumbers. In particular, the CH_2 asymmetric stretch in the perpendicularly polarized spectrum undergoes a shift of 3 cm^{-1} while in the parallel polarized spectra no

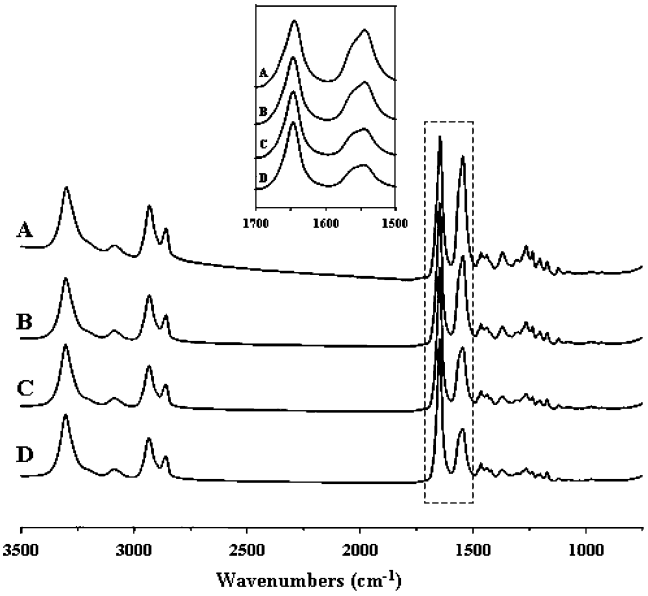

Figure 5. Perpendicularly polarized FT-IR spectra of nylon-6 nanofibers electrospun onto the rotating mandrel collector with a linear velocity of (A) 0, (B) 300, (C) 600, and (D) 900 m/min.

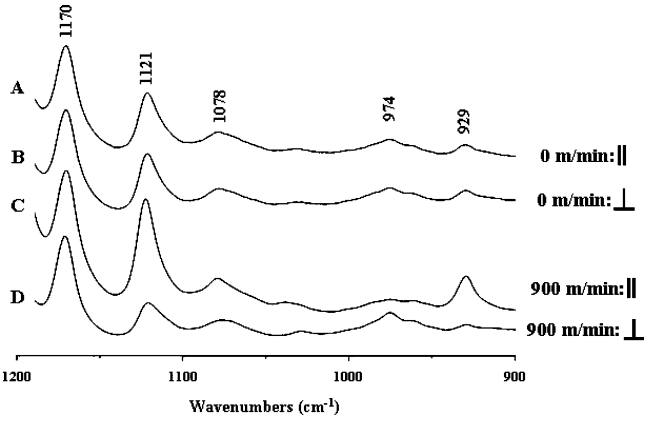

Figure 6. Polarized FT-IR spectra of PA 6 nanofibers electrospun onto the rotating mandrel collector with a windup speed of (A) 0 m/min: parallel polarization (electric field oriented parallel to fiber axis); (B) 0 m/min: perpendicular polarization; (C) 900 m/min: parallel polarization; and (D) 900 m/min: perpendicular polarization.

Table 2. Dichroic Ratio of Different Vibrational Bands

	linear velocity of rotating collector (m/min)			
band (cm^{-1})	0	300	600	900
3300	1.01	0.68	0.84	0.58
1645	1.01	0.69	0.85	0.61
1544	1.03	1.53	3.27	3.63
1121	1.02	1.58	3.45	3.68
974	1.00	0.64	0.72	0.55
929	1.00	1.94	5.81	6.03

shift is observed. This suggests that there is a small increase in the α-content and also that the orientation of the α-form is more substantial. The CC stretching band at 1121 cm^{-1} is assigned to the amorphous phase,[16] and its dichroic ratio (>1) indicates that there is net orientation of the amorphous polymer along the fiber axis with an increase in the linear velocity of the rotating mandrel even though in less extent compare to the α-form (see Table 2).

In order to support these results, DSC measurements were carried out, and the resulting melting temperature, heat of fusion, and crystallinity from each sample are summarized in Table 3. As demonstrated from the DSC results, the crystallinity of the

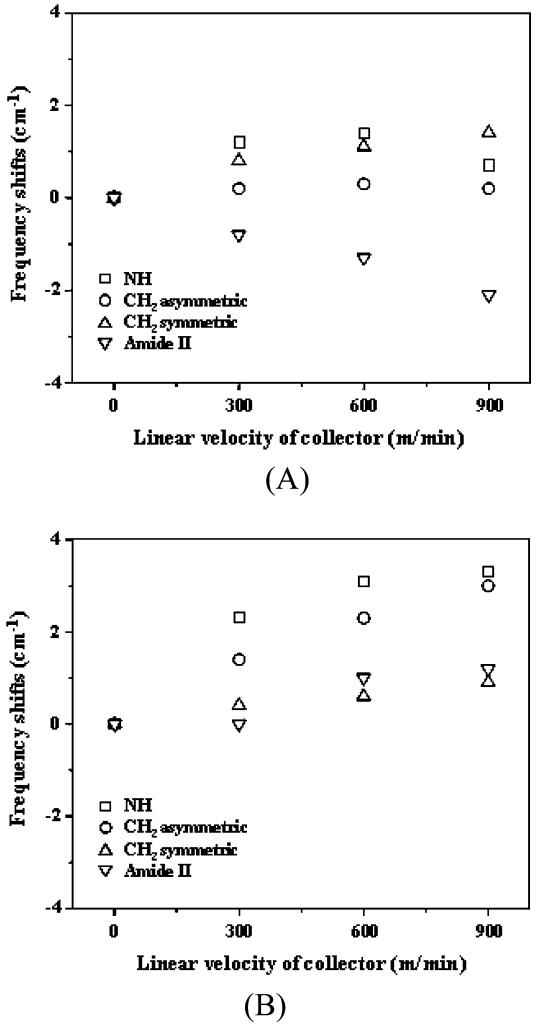

Figure 7. Various band shifts as a function of a linear velocity of the rotating mandrel collector: (A) parallel and (B) perpendicular polarization.

Table 3. DSC Data for Electrospun Nylon-6 Nanofibers with Different Linear Velocities of the Rotating Mandrel

linear velocity of rotating mandrel (m/min)	melting temp[a] (°C)	heat of fusion (J/g)	crystallinity (%)
0	223.9 (214.2)	77.2	32.2
300	226.0 (215.3)	82.9	34.5
600	224.4 (215.4)	83.3	34.7
900	224.6 (216.4)	82.2	34.3

[a] Values in parentheses indicate the melting temperature of shoulder endothermic peak.

sample obtained at a mandrel linear velocity of 300 m/min is slightly higher than that obtained at 0 m/min. For higher linear velocities of the mandrel surface, there is no further increase in cyrstallinity. Hence, these results are in good agreement with the FT-IR spectra showing the same trend.

Another interesting aspect in the FT-IR analysis of H-bonded amide polymers is to evaluate the changes in crystalline structure due to changes in the H-bond strength caused by stress, deformation, etc. Many studies on nylon-6 exploring this have been reported but a clear picture is still not well-defined. In fact, NMR studies on crystalline forms of nylon-6 by Okada et al.[2] showed that the H-bond is stronger in the γ-form compared to the α-form, but other studies[21,22] argue exactly the opposite, that the H-bond is much stronger in the α-form due to a closer packing of the nylon-6 chains. Any change in the H-bond will

affect many vibrational modes, including the NH stretching vibration, amide I, and amide II. However, it is important to note that the amide I and amide II are complex vibrational modes, involving displacement of multiple molecular groups, and that the NH stretching vibration is a very broad band that has contributions from both amorphous and crystalline phases. More specifically, the NH stretching vibration is not a simple and direct indication of the hydrogen-bond strength.[22] Nevertheless, our data suggest that there is a weakening in the H-bond with an increase in the linear velocity of the rotating collector at least in the direction parallel to the machine direction. This cannot be easily correlated to conformational changes. The IR data show a shift of the amide II peak at 1543 cm^{-1} to lower frequency as the linear velocity increases from 0 to 900 m/min for parallel polarized spectra, while there is a slight shift to higher frequency observed for the same band in the perpendicular polarized spectra (Figure 7). Moreover, peak intensity of the 1662 cm^{-1} high-frequency shoulder on the amide I band (attributed mainly to the free H-bond carbonyl stretching vibration) in the parallel polarized spectra increases with the linear velocity of the rotating mandrel. In addition, the full width at half-maximum (fwhm) of the NH stretching vibration increases, too. The observed low-frequency shift of the amide II is believed to be due to a weakening of the H-bond.[22] Correspondingly, the appearance of the band for free carbonyl stretching indicates that the average strength of the H-bond is diminishing while the fwhm of the NH band indicates that there is a broader distribution of H-bond strengths. It is also possible that the small shift of the amide II to higher frequency in the perpendicular polarized spectra could be attributed to a strengthening of the H-bond, but there is, currently, no other supporting data for this interpretation. Actually, we always observe an upshift of the NH stretching mode both in the parallel and the perpendicular polarized spectra with an increase in the linear velocity of the rotating mandrel but as already mentioned the frequency could be affected also by angles of H-bonds and their distribution. The fact that in the perpendicular polarized spectrum the fwhm is always narrower is indicative of the fact that the distribution of NH stretching vibrations is less disperse in this direction most likely due to the slightly higher crystallinity.

Conclusions

Electrospun, macroscopically aligned, molecularly oriented nylon-6 nanofibers have been prepared by controlling the linear velocity of a rotating collector. Molecular orientation was characterized by polarized FT-IR. In the case of randomly deposited nylon-6 nanofibers, the parallel and perpendicularly polarized FT-IR spectra are identical, indicating an isotropic distribution of polymer backbones. On the other hand, the polarized FT-IR spectra of electrospun nylon-6 nanofibers, deposited onto a rotating collector with linear velocity of above 300 m/min, showed differences in the relative intensity of bands, indicating that molecular orientation of polymer chains had occurred parallel to the fiber axis. As demonstrated by SEM, the decrease in the average fiber diameter indicates that fibers were stretched and aligned along the fiber axis. In the initial windup stage, crystallinity content increased significantly due to drawing of the fibers along the fiber direction. For higher mandrel linear speeds, there is no substantial increase in the crystallinity as indicated by DSC. Consequently, it is most likely that at the lower (300 m/min) mandrel linear velocities α-form crystals form mainly from the amorphous phase, but later the small increase in crystallinity observed at the higher mandrel speed (300 m/min and above) is at the expense of the γ-form.

Acknowledgment. We acknowledge the support of NASA (Genetically Engineered Polymers Grant 372116), NSF EPSCoR (Grants DBIO312163 and DBIO422163), and NSF DMR for support of this work. Hak-Yong Kim acknowledges the Korean Ministry of Education & Human Resources Development, through the Center for Healthcare Technology Development, for financial support during these studies.

References and Notes

(1) Alger, M. In *Polymer Science Dictionary*, 2nd ed.; Chapman & Hall: London, 1997.
(2) Okada, A.; Kawasumi, M.; Tajima, I.; Kuruachi, T.; Kamigaito, O. *J. Appl. Polym. Sci.* **1989**, *37*, 1363−1371.
(3) Doshi, J.; Reneker, D. H. *J. Electrostat.* **1995**, *35*, 151−160.
(4) Fong, H.; Chun, I.; Reneker, D. H. *Polymer* **1999**, *40*, 4585−4592.
(5) Lee, K. H.; Kim, H. Y.; Khil, M. S.; Ra, Y. M.; Lee, D. R. *Polymer* **2003**, *44*, 1287−1294.
(6) Huang, Z.-M.; Zhang, Y.-Z.; Kotaki, M.; Ramakrishna, S. *Compos. Sci. Technol.* **2003**, *63*, 2223−2253.
(7) Subbiah, T.; Bhat, G. S.; Tock, R. W.; Parameswaran, S.; Ramkumar, S. S. *J. Appl. Polym. Sci.* **2005**, *96*, 557−569.
(8) Matthews, J. A.; Wnek, G. E.; Simpson, D. G.; Bowlin, G. L. *Biomacromolecules* **2002**, *3*, 232−238.
(9) Teo, W. E.; Kotaki, M.; Mo, X. M.; Ramakrishna, S. *Nanotechnology* **2005**, *16*, 918−924.
(10) Fennessey, S. F.; Farris, R. J. *Polymer* **2004**, *45*, 4217−4225.
(11) Katta, P.; Alessandro, M.; Ramsier, R. D.; Chase, G. G. *Nano Lett.* **2004**, *4*, 2215−2218.
(12) Kameoka, J.; Orth, R.; Yang, Y.; Czaplewski, D.; Mathers, R.; Coates, G. W.; Craighead, H. G. *Nanotechnology* **2003**, *14*, 1124−1129.
(13) Li, D.; Wang, Y.; Xia, Y. *Adv. Mater.* **2004**, *16*, 361−366.
(14) Kakade, M. V.; Givens, S.; Gardner, K.; Lee, K. H.; Chase, D. B.; Rabolt, J. F. *J. Am. Chem. Soc.* **2007**, *129*, 2777−2782.
(15) Arimoto, H. *J. Polym. Sci., Part A* **1964**, *2*, 2283−2295.
(16) Vasanthan, N. *Appl. Spectrosc.* **2005**, *59*, 897−903.
(17) Vasanthan, N.; Salem, D. R. *J. Polym. Sci., Part B: Polym. Phys.* **2001**, *39*, 536−547.
(18) Fornes, T. D.; Paul, D. R. *Polymer* **2003**, *44*, 3945−3961.
(19) Koski, A.; Yim, K.; Shivkumar, S. *Mater. Lett.* **2004**, *58*, 493−497.
(20) Reneker, D. H.; Yarin, A. L.; Fong, H.; Koombhongse, S. *J. Appl. Phys.* **2000**, *87*, 4531−4547.
(21) Dasgupta, S.; Hammond, W. B.; Goddard, W. A., III *J. Am. Chem. Soc.* **1996**, *118*, 12291−12301.
(22) Loo, L. S.; Gleason, K. K. *Macromolecules* **2003**, *36*, 6114−6126.

MA701927W